



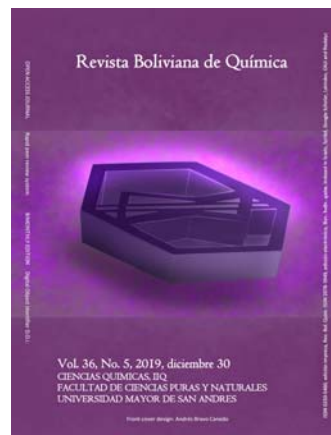
## SYNTHESIS OF ZSM-5 ZEOLITE USING DIATOMITE AS PRECURSOR; ITS APPLICATION IN THE METHANOL TO HYDROCARBONS PROCESS (MTH)

## SÍNTESIS DE ZEOLITA ZSM-5 UTILIZANDO DIATOMITA COMO PRECURSOR; SU APLICACIÓN EN EL PROCESO DE METANOL A HIDROCARBUROS (MTH)

Received 10 15 2019  
Accepted 12 25 2019  
Published 12 30 2019

Vol. 36, No.5, pp. 198-209, Nov./Dic.2019  
Revista Boliviana de Química

36(5), 198-209, Nov./Dec. 2019  
Bolivian Journal of Chemistry  
DOI: 10.34098/2078-3949.36.5.2



Full original article

Peer-reviewed

Ronald M. Lara Prado<sup>1,\*</sup>, Dayana M. Capcha Vargas<sup>1</sup>, Yamil Acho Sarzuri<sup>2</sup>, Edgar Cárdenas<sup>1,3</sup>, Gustavo García<sup>1</sup>, Saúl Cabrera M.<sup>1,2</sup>, Luis López N.<sup>1,2</sup>

<sup>1</sup>Instituto de Investigaciones Químicas IIQ, Área de Ciencia de Materiales, Catálisis y Petroquímica, Facultad de Ciencias Puras y Naturales FCPN, Universidad Mayor de San Andrés UMSA, P.O. Box 303, Calle Andrés Bello s/n-Edificio IIQ, Campus Universitario Cota Cota, Phone +59122795878, La Paz, Bolivia, <http://cienciasquimicas.umsa.bo/>

<sup>2</sup>Instituto del Gas Natural IGN, Universidad Mayor de San Andrés UMSA, P.O. Box 303, Calle Andrés Bello s/n-Edificio IIQ, Campus Universitario Cota Cota, Phone +59122795878, La Paz, Bolivia

<sup>3</sup>Chemical Technology, Luleå University of Technology, 971 87 Luleå, Sweden

**Keywords:** *Methanol to hydrocarbons, Dimethyl ether, Olefins, Diatomite, H-ZSM-5.*

**Palabras clave:** *Metanol a hidrocarburos, Éter dimetílico, Olefinas, Diatomita, H-ZSM-5.*

### ABSTRACT

Zeolite H-ZSM-5 is widely applied in the petrochemical industry, such as the synthetic process of methanol to hydrocarbons (methanol to hydrocarbons MTH). ZSM-5 zeolite is currently obtained through reagents and expensive processes, being available only a few cheaper alternative routes. In the present investigation, zeolite H-ZSM-5 was obtained from natural diatomite, then characterized, and finally tested in the synthetic MTH process. The natural diatomite was treated with sulfuric acid to perform hydrothermal synthesis with tetrapropyl ammonium hydroxide (TPA-OH). As a result, the H-ZSM-5 zeolite obtained had a Si / Al molar ratio of 23, it exhibited high thermal stability and showed Lowry-Brønsted and Lewis acid sites. The application of this zeolite in the MTH reaction showed a methanol conversion of 88%. The products were: dimethyl ether (DME) in 40%, olefins (mostly ethylene and propylene) in 40% and others in 20%. The reaction conditions were: 300 ° C, 1.2L<sub>metanol</sub>/g<sub>cat</sub>·h at atmospheric pressure (0.65 bar). The selectivity of the products can be modified in such a way that DME can be



obtained preferentially, up to > 93%, by changing the operating conditions (temperature and space velocity). The use of natural diatomite as a starting material for the preparation of the zeolite H-ZSM-5 represents an attractive route and deserves further investigation for its application and development.

\*Corresponding author: [ronaldlara49@gmail.com](mailto:ronaldlara49@gmail.com)

## RESUMEN

La zeolita H-ZSM-5 es ampliamente aplicada en la industria petroquímica como por ejemplo en el proceso sintético de metanol hasta hidrocarburos (methanol to hydrocarbons MTH). La zeolita ZSM-5 es obtenida a través de reactivos y procesos costosos, existiendo pocas rutas alternativas que sean más económicas. En la presente investigación, zeolita H-ZSM-5 fue obtenida a partir de diatomita natural, seguidamente caracterizada, y finalmente probada en la proceso sintético MTH. La diatomita natural fue tratada con ácido sulfúrico para la realización de la síntesis hidrotermal con hidróxido de tetrapropil amonio (TPA-OH). Como resultado, la zeolita H-ZSM-5 obtenida tuvo una relación molar Si/Al de 23, presentó estabilidad térmica alta y sitios ácidos Lowry-Brønsted y Lewis. La aplicación de esta zeolita en la reacción MTH, presentó una conversión de metanol del 88 %. Los productos fueron: dimetil éter (DME) en un 40 %, olefinas (mayoritariamente etileno y propileno) en un 40% y otros en un 20 %. Las condiciones de reacción fueron de: 300°C, 1,2L<sub>metanol</sub>/g<sub>cat</sub> a presión atmosférica (0.65 bar). La selectividad de los productos puede ser modificada de tal forma que pueda obtenerse DME de manera preferencial, hasta > 93 %, mediante el cambio de las condiciones de operación (temperatura y velocidad espacial). El uso de diatomita natural como material de partida para la preparación de la zeolita H-ZSM-5 representa una ruta atractiva y merece mayor investigación para su aplicación y desarrollo.

## INTRODUCTION

The methanol to hydrocarbons (MTH) process is a good petrochemical option for the production of clean fuels such as gasoline, diesel or dimethyl ether (DME), with similar properties as compared with fuels obtained from crude oil [1,2]. Other products obtained from the MTH process are chemicals such as ethylene and propylene, which are precursors highly demanded in the polymer industry [3,4]. In general, the MTH process uses different kind of zeolites being one of the most common the H-ZSM-5 [5,6]. This zeolite is commonly synthesized from sodium silicate, aluminum nitrate and tetra propyl ammonium hydroxide (TPA-OH) as structure directional agents (SDA) under LBASic pH conditions [7,8]. The use of less expensive raw materials could reduce the overall synthesis cost of H-ZSM-5 zeolite. One alternative for the H-ZSM-5 zeolite synthesis is the use of natural diatomite, where the diatomite is an attractive source of silica and aluminum and it has the advantage of being a more environmentally friendly process [9]. A proper pre-treatment of diatomite not only reduces the amount of impurities such as Ca, Fe and Mg that are usually present in natural diatomites [10], but also it allows to reach a proper Si/Al ratio prior zeolite synthesis [11].

In the present work, the preparation of H-ZSM-5 zeolite using natural diatomite treated with sulfuric acid and subsequent hydrothermal synthesis with TPA-OH, was studied. The zeolite was characterized by XRD, TPD, SEM, ICP, TGA-DSC from which a pure ZSM-5 was identified, trace amounts of metals, high thermal stability, strong Lowry-Brønsted and Lewis acid sites and a Si/Al molar ratio of 23. This zeolite showed high selectivity toward dimetil ether (>97%) and high conversion (>68%) in the MTH process.

## RESULTS AND DISCUSSION

### *Characterization of H-ZSM-5 obtained from diatomite*

#### *Inductively coupled plasma-sector field mass spectrometry (ICP-SFMS)*

The results from ICP-SFMS show that the treatment of diatomite with sulfuric acid considerably reduces the concentration of metallic elements such as Al, Ca, Fe, K, Mg, Na, as it is shown in Table 1. Comparing with a previous work [11] where diatomite was treated in a reflux system with hydrochloric acid at 115 °C for 150 minutes, the reduction of the concentration of Al, Na, K, Mg and Na are practically in the same range, with the exception of



Ca and Fe. Also the  $\text{SiO}_2/\text{Al}_2\text{O}_3$  ratio is in the same range: 44 from hydrochloric acid treatment and 49.4 from sulfuric acid treatment. The Si/Al ratio is a very important parameter for the synthesis of zeolites, since the ratio defines its application as selective a catalyst in several petrochemical processes. For example in the MTH process, the zeolite H-ZSM-5 typically has a Si/Al ratio in the range of 3 -  $\infty$  [12]. The H-ZSM-5 zeolite obtained from diatomite has a Si/Al ratio equal to 46.3, see Table 1.

**Table 1.** Composition (in mole %) of diatomite, acid treated diatomite and H-ZSM-5 zeolite by ICP-SFMS

| Elemental Composition                          | Natural Diatomite, % | Acid treated Diatomite, % | H-ZSM-5, %    |
|--|----------------------|---------------------------|---------------|
| Si ( $\text{SiO}_2$ )                          | 59,0 (70.8)          | 93.4 (95.9)               | 91.1 (94.8)   |
| Al ( $\text{Al}_2\text{O}_3$ )                 | 9.8 (5.9)            | 3.8 (1.9)                 | 3.9 (2.1)     |
| Ca ( $\text{CaO}$ )                            | 3.7 (4.4)            | 1.0 (1.1)                 | 0.8 (0.9)     |
| Fe ( $\text{Fe}_2\text{O}_3$ )                 | 1.3 (0.8)            | 0.1 (0.1)                 | 0.1 (0.1)     |
| K ( $\text{K}_2\text{O}$ )                     | 2.4 (1.4)            | 0.8 (0.4)                 | 1.8 (0.9)     |
| Mg ( $\text{MgO}$ )                            | 4.1 (4.9)            | 0.2 (0.2)                 | 0.2 (0.2)     |
| Na ( $\text{Na}_2\text{O}$ )                   | 19.7 (11.8)          | 0.8 (0.4)                 | 2.0 (1.0)     |
| Total  | 100.0 (100.0)        | 100.0 (100.0)             | 100.0 (100.0) |
| Si/Al ( $\text{SiO}_2/\text{Al}_2\text{O}_3$ ) | 6.0 (12.1)           | 24.7 (49.4)               | 23.4 (46.3)   |

#### X-ray diffraction (XRD)

##### a) Sulfuric acid treatment of the natural diatomite

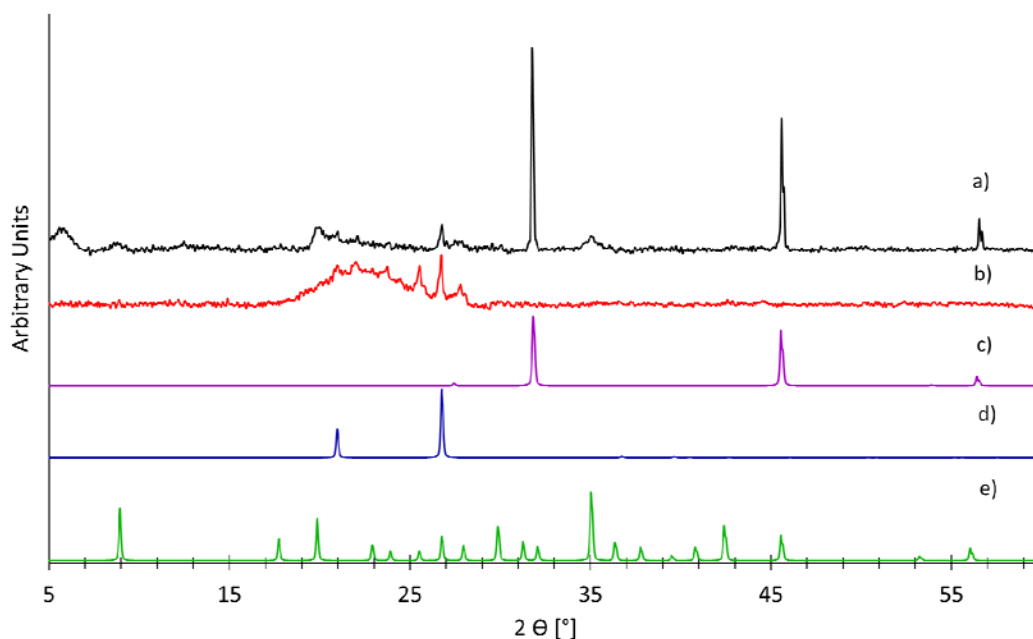


**Fig. 1.** XRD diffractograms: a) Pure Diatomite, b) Acid treated Diatomite, c) Reference pattern of NaCl Halite (PDF-00-001-0993), d) Reference Pattern of  $\text{SiO}_2$  Quartz (PDF-01-083-2466) and e) Reference pattern of  $\text{KAl}_2(\text{AlSi}_3\text{O}_{10})(\text{OH})_2$  Muscovite (PDF-00-001-1098)

From the XRD diffractogram of pure diatomite (Fig. 1a) the following structure can be identified:  $\text{SiO}_2$  as Quartz (Fig. 1d), NaCl as Halite (Fig. 1c) and  $\text{KAl}_2(\text{AlSi}_3\text{O}_{10})(\text{OH})_2$  as Muscovite (Fig. 1e). As a consequence of the acid



treatment of diatomite, the NaCl and  $KAl_2(AlSi_3O_{10})(OH)_2$  signals totally disappear while the signals of Quartz are affected in minor degree.

#### b) Synthesis of H-ZSM-5 from acid treated diatomite

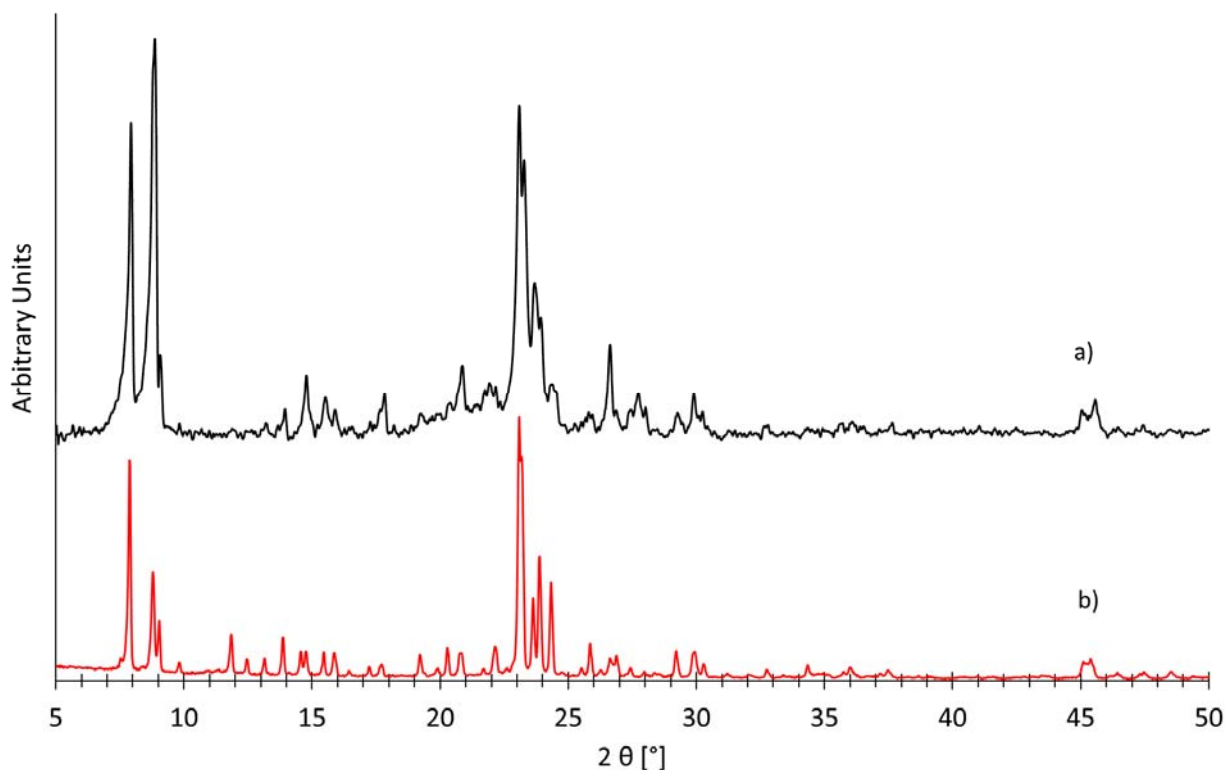


Fig. 2. XRD diffractograms of: a) H-ZSM-5 synthesized from diatomite and b) Reference pattern of H-ZSM-5 zeolite (PDF-042-0024)

After a hydrothermal synthesis using the acid treated diatomite and TPA-OH, the H-ZSM-5 zeolite is obtained (Fig. 2a), as identified with the diffraction angles at  $2\theta = 7.4^\circ$  to  $9.2^\circ$  and  $22.0^\circ$  to  $25.0^\circ$  which correspond to the H-ZSM-5 structure (Fig. 2b). This indicates that the use of diatomite as resource of Si and Al is adequate for the synthesis of H-ZSM-5. Moreover, Si and Al from diatomite can form oligomers that could interact in a simpler way with the directional agent TPA-OH, which facilitates the synthesis of H-ZSM-5 as suggested in the literature [13]. The crystallinity degree and average crystallite size of the H-ZSM-5 zeolite are 47.0 % and 69,2 nm respectively.

#### Scanning electronic microscopy (SEM)

In the SEM image of the natural diatomite (Fig. 3a) large particles can be observed with the typical shape of diatomite biogenic sediments. The obtained H-ZSM-5 zeolite presents large elongated ellipsoidal particles with sizes between  $4.5\ \mu\text{m}$  to  $10.9\ \mu\text{m}$  (Fig. 3 b). Moreover, the zeolite particles are formed by agglomerates of nano-crystals as observed in Fig. 3c, which is commonly obtained at high aluminum content [14]. The zeolite nano-crystal size distribution is shown in Fig. 3d where the average particle size is 63 nm, this value is in agreement with the particle calculated from the Scherrer equation equal to 69 nm, (see section 2.1.2).

The DTGA profiles show a high thermal stability up to  $800^\circ\text{C}$  for all the studied materials; natural diatomite (Fig. 4a), acid treated diatomite (Fig. 4b) and for the final H-ZSM-5 zeolite (Fig 4c). For all the cases a loss of weight is found below  $200^\circ\text{C}$ , which corresponds to the elimination of adsorbed water; 14.9 wt % in the natural diatomite, 8.8 wt % in the acid treated diatomite and 3.3 wt % in the H-ZSM-5.

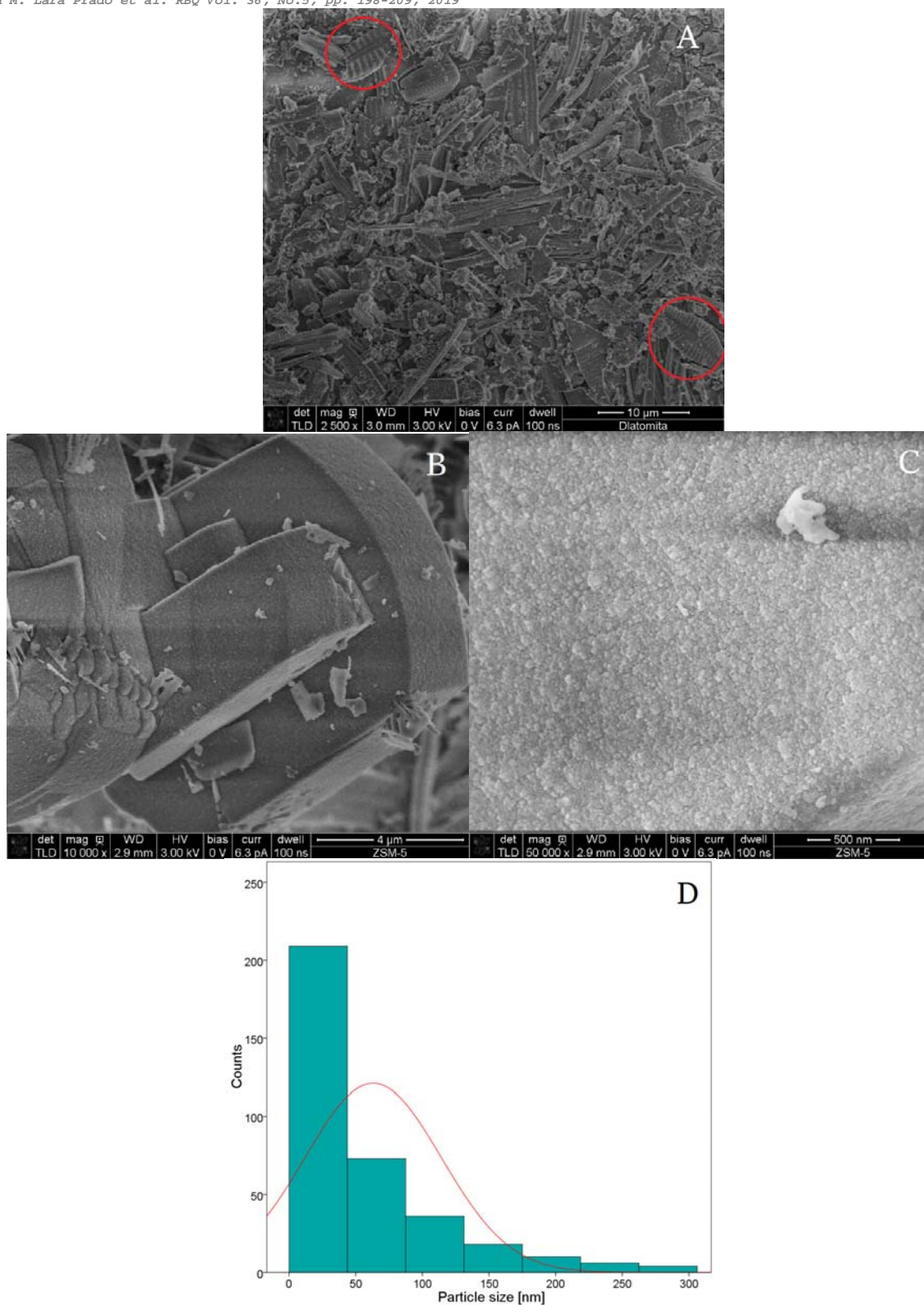


Fig. 3. SEM images of a) Natural Diatomite b, c) obtained H-ZSM-5 zeolite, and d) Zeolite nano-crystal size distribution. Thermal gravimetric analysis (TGA)

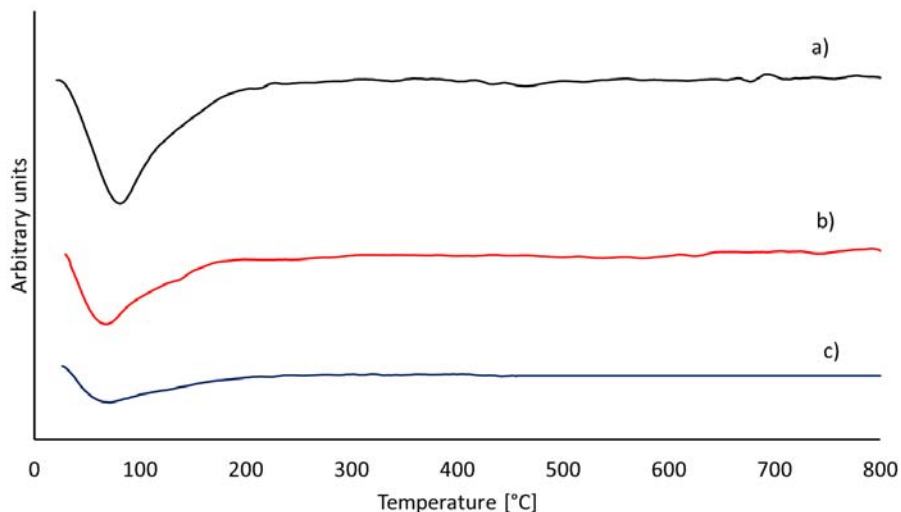


Fig. 4. DTGA profile of: a) Pure Diatomite, b) Acid treated Diatomite and c) obtained H-ZSM-5 zeolite

#### Ammonia temperature programmed desorption ( $\text{NH}_3$ -TPD)

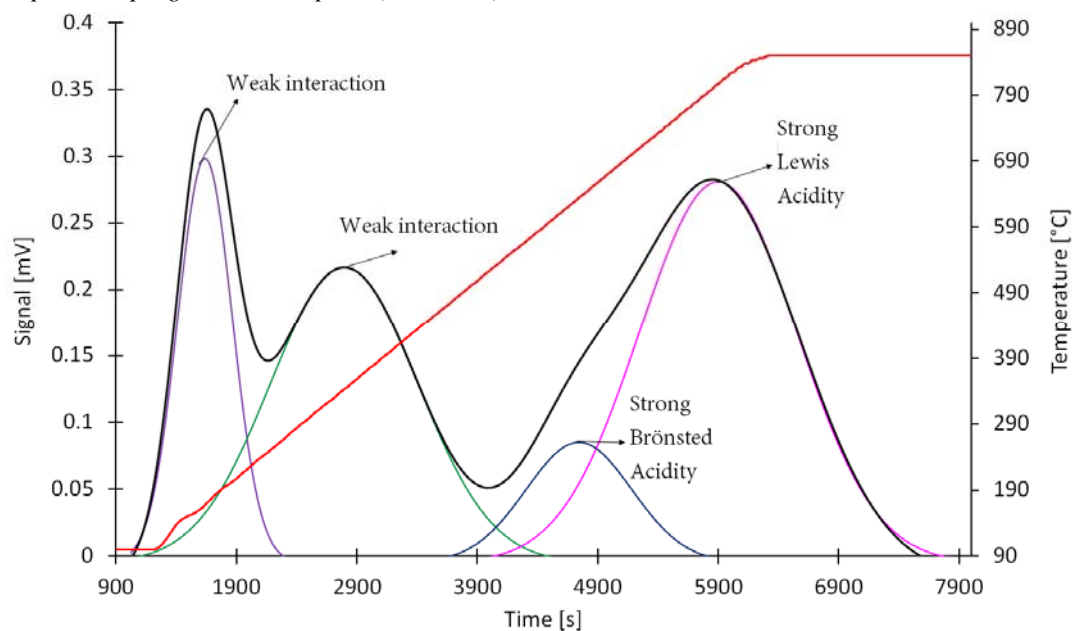


Fig. 5.  $\text{NH}_3$ -TPD profile of the obtained H-ZSM-5 zeolite

TPD profile of the obtained H-ZSM-5 zeolite show signals in the range of 90 °C to 850 °C (Fig. 5), in agreement with the literature for the ZSM-5 zeolite [15-17]. Four deconvoluted signals are assigned in the following range of temperatures; from 100 °C to 280 °C, from 100 °C to 550 °C, from 400 °C to 720 °C, and from 550 °C to 850 °C. The first and second deconvoluted signals can be assigned to the physically  $\text{NH}_3$  desorption from  $\text{NH}_4^+n\text{NH}_3$  species with  $n = 2$  and  $n = 1$ , respectively, in concordance with the proposed model by Takeuchi et. al. and Lónyi et. al. [15,18]. In addition, the second de-convoluted signal can have a contribution of  $\text{NH}_3$  desorbed from week Lewis acid sites [19-21]. This week Lewis acid site can be originated by  $\text{Na}^+$  which remains in the final ZSM-5 zeolite (see ICP results, Section 2.1.1.).

The third and fourth deconvoluted signals can be assigned to desorption of  $\text{NH}_3$  from strong acid sites, either a Lowry-Brønsted acid site (LBAS) or a Lewis acid site (LAS) [22]. In order to distinguish between LBAS and LAS,



an experimental test was carried out where the ZSM-5 was treated with 1 M hydrochloric acid so the extra framework aluminums (EFAL) should preferentially be eliminated and thus the signal of LAS be diminished [23-25]. After the HCl treatment of H-ZSM-5, about 80 % of the intensity corresponding to the fourth deconvoluted signal was diminished while the intensity of the third deconvoluted signal was diminished only 20 %. Thus, we assigned the third deconvoluted signal to LBAS and the fourth deconvoluted signal due to LAS. The LBAS is normally formed by the presence of H<sup>+</sup> in the zeolite, which at the same time compensate the charge deficiency produced by the intrusion of tetrahedral aluminum into the silicon crystalline structure. [22] While the LAS can be originated by two mechanisms; first, similarly to H<sup>+</sup> but with a different cation (e.g. Na<sup>+</sup> and K<sup>+</sup>), and second, by cationic species such as [AlO]<sup>+</sup> segregated in the form of EFAL [26-27].

**Table 2.** Acidity quantification of the H-ZSM-5 zeolite

| Type of interaction                    | Deconvoluted Signal | Maximum temperature, °C | Mole NH <sub>3</sub> /Kg <sub>zeolite</sub> |
|--|---------------------|-------------------------|---|
| NH <sub>3</sub> physisorption (n=2)*   | I                   | 175                     | 0.15  |
| NH <sub>3</sub> physisorption (n=1)*   | II                  | 346                     | 0.29  |
| Strong Brønsted acid sites (LBAS)      | III                 | 638                     | 0.09  |
| Strong Lewis acid sites (LAS)          | IV                  | 808                     | 0.40  |
| Total Acidity (LBAS + LAS)             | III,IV              | -                       | 0.49  |
| Mole Al/Kg <sub>zeolite</sub> from ICP |                     | -                       | 0.57  |

\* As model proposed by Takeuchi. [18]

The quantification of total acidity from TPD, in terms of the amount absorbed of NH<sub>3</sub> for the H-ZSM-5 zeolite was 0.49 mole NH<sub>3</sub>/Kg<sub>zeolite</sub>, (see Table 2), which is in agreement with those reported in the literature [28,29]. Furthermore, this value is close to the total Al content in the zeolite; 0.57 mole Al/Kg<sub>zeolite</sub> found from ICP (see above), suggesting that one NH<sub>3</sub> molecule is adsorbed in one acid site which is generated by one aluminum. In addition, some Al species can be trapped into the zeolite's pores being inaccessible for interacting with NH<sub>3</sub> molecules.

### Catalytic performance of the H-ZSM-5 zeolite in the MTH reaction

The obtained H-ZSM-5 zeolite was evaluated in the MTH reaction at typical conditions: space velocities (SV) from (1.2L/g<sub>cat</sub>h) to 15L/g<sub>cat</sub>h), temperature from (240°C to 300°C) and atmospheric pressure (0.65 bar). At the beginning of the MTH reaction it was observed an induction period of about 1 hour, where the methanol conversion gradually increased up to a pseudo-stationary state. This period is provoked by the formation and progressive adsorption of intermediary species over the acid sites of the zeolite as described by the hydrocarbon pool mechanism [30-32]. After reaching the pseudo-stationary state, the effect of SV was evaluated in the period A and B and the effect of temperature was evaluated in the period C, as indicated in Table 3.

#### a) Effect of the space velocity

In period A, the principal products were olefins, mostly ethylene and propylene and DME, and minor amounts of paraffins C<sub>1</sub> to C<sub>5</sub> and higher (C<sub>>5</sub>), and the methanol conversion was of 88 %, close to the equilibrium conversion, namely about 100 %. At higher GHSV, period B, the product selectivity changes considerably where the main product becomes DME, superior to 95 % and in minor amounts of olefins, less than 5 %, and the methanol conversion decreases in a remarkable diminution until reaching a 54 %.

The products obtained in period A can be explained by different reaction mechanisms, one of those is the reaction pathway suggested by Stöcker [30] (see Fig. 6), where the methanol is dehydrated by the capture of a proton from a strong Lowry-Brønsted acid site to form intermediary cationic species, this species remains close for charge compensation. A second molecule of methanol interacts with the cationic species to form DME and regenerate the strong Lowry-Brønsted acid site. DME can react with another cationic species to form light olefins. Then the interaction between light olefins gives larger compounds such as larger olefins and paraffins. At higher GHSV such as the period B there are minor interactions between reactive species and active sites due to a minor residence time, so, larger compounds are less favored maximizing the selectivity to DME.



Table 3. MTH results with the obtained H-ZSM-5 zeolite

| Reaction condition                             | Period A:<br>T = 300 °C, P = 0.65 bar<br>GHSV = 1.2 L <sub>methanol</sub> /g <sub>cat</sub> h | Period B:<br>T = 300° C, P = 0.65 bar<br>GHSV = 15 L <sub>methanol</sub> /g <sub>cat</sub> h | Period C:<br>T = 240 °C, P = 0.65 bar<br>GHSV=1.2L <sub>methanol</sub> /g <sub>cat</sub> h |
|--|---|--|--|
| Time on stream (TOS)                           | 7 h   | 5 h  | 3 h  |
| Methanol conversion $X_{\text{MeOH}}$ (%)      | 88.2 ± 1.9  | 54.0 ± 0.1   | 65.7 ± 1.4   |
| Product selectivity S, (%)                     |   |  |  |
| Ethylene [S <sub>C2</sub> <sup>=</sup> ]       | 22.2 ± 0.9  | 1.9 ± 0.1  | 0.9 ± 0.5  |
| Propylene [S <sub>C3</sub> <sup>=</sup> ]      | 19.2 ± 0.6  | 2.2 ± 0.2  | 0.9 ± 0.6  |
| Propane [S <sub>C3</sub> ]                     | 1.7 ± 0.2   | -  | -  |
| Dimethyl ether [S <sub>DME</sub> ]             | 39.5 ± 1.9  | 95.9 ± 0.3   | 93.4 ± 1.1   |
| Iso Butane [S <sub>i-C4</sub> ]                | 2.4 ± 0.2   | -  | 4.8 ± 0.1  |
| Ter-Butane [S <sub>t-C4</sub> ]                | 3.4 ± 0.3   | -  | -  |
| Butane [S <sub>n-C4</sub> ]                    | 2.9 ± 0.2   | -  | -  |
| Cis Butene [S <sub>Cis-C4</sub> <sup>=</sup> ] | 1.3 ± 0.6   | -  | -  |
| Aromatics [S <sub>C&gt;5</sub> <sup>+</sup> ]  | 7.4 ± 1.5   | -  | -  |

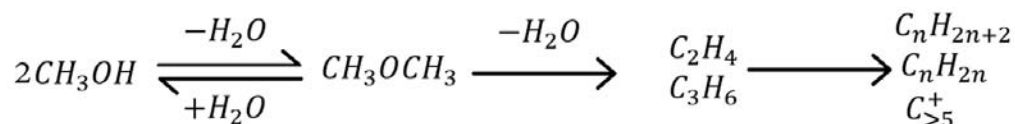


Fig. 6. Reaction pathways for the MTH reaction (adapted from Stöcker [30] Copyright (1999), with permission from Elsevier)

#### b) Effect of the temperature

After changing the reaction temperature from 300°C to 240°C, the product selectivity is considerably changed, the DME becomes the main product (>94 %) and minor amounts of olefins and hydrocarbons (<6 %) are formed (see period A and C in table 3). The methanol conversion is of 65 % and the equilibrium conversion at this temperature is 100%. Lower temperatures reduce the methanol conversion and changes the product selectivity according to the reported in the literature [33].

## EXPERIMENTAL

### Synthesis of H-ZSM-5 zeolite

#### Acid treatment of diatomite

The diatomite used in the present work was collected at the locality of Murmuntani in Potosí, Bolivia at 4067 m.a.s.l. A 6 M solution of sulfuric acid (Merck p.a.) was prepared. The diatomite was treated with the a 6 M sulfuric acid solution under hydrothermal conditions in an oven at 100°C during 24h. Subsequently, the suspension was quenched and washed with distillate water until pH ≈ 7. The solid obtained was separated by filtering and dried overnight at 100 °C.



The synthetic mixture was prepared by using the acid treated diatomite and distillate water, sodium hydroxide (Merck p.a.) and TPA-OH (Merck reactive 1M solution) as SDA. The molar ratios in the synthesis mixture were:  $\text{Na}_2\text{O}/\text{SiO}_2 = 0.18$ ;  $\text{SiO}_2/\text{Al}_2\text{O}_3 = 49.4$ ;  $\text{SiO}_2/\text{TPA-OH} = 3.5$ ;  $\text{H}_2\text{O}/\text{SiO}_2=30$ , the mixture was stirred for 24 hours at room temperature and the pH adjusted at 11 with 1M hydrochloric acid. The mixture was then hydrothermally treated in a Teflon stainless steel autoclave in a pre-heated oven at 170 °C for 48 hours. Subsequently, the suspension was quenched and washed with distillate water until pH  $\approx 7$ . Finally, the obtained solid was dried at 100 °C overnight and calcinated at 550 °C for 8 hours.

#### *NH<sub>4</sub><sup>+</sup> ion exchange of ZSM-5 zeolite*

The protonated form of the zeolite (H-ZSM-5) was obtained by mixing it with ammonium nitrate 1 M in a reflux system at 80 °C for 12 hours. The zeolite to ammonium nitrate weight ratio was 1:12. Subsequently, the solid was separated by filtering and washed with distillate water. Finally, the zeolite was dried at 100 °C overnight and calcinated for 8 hours at 550 °C. This procedure was carried out twice.

#### *Characterization techniques*

The elemental composition of diatomite, acid treated diatomite, and H-ZSM-5 zeolite was quantified with Inductively Coupled Plasma-Sector Field mass spectrometry (ICP-SFMS). 0.1 g of the sample was fused with 0.4 g of LiBO<sub>2</sub> and dissolved in nitric acid. Each sample was analyzed thrice.

The identification of crystalline phases, crystallinity degree and the average crystal size of the samples was determined by X-ray diffraction (XRD) technique on a PANalytical X-ray Diffractometer with an X-ray tube of copper ( $K_{\alpha} = 1.54 \text{ \AA}$ ) and Xcelerator detector. The operational conditions applied to X-ray tube was 40 mA y 40 kV. The analysis range was from 5° to 60°, 2 $\theta$  Bragg degrees.

The crystallinity degree (Eq. 1) [34] was assessed by calculating the area under the principal peaks in the 2 $\theta$  region between 22.0° to 25.0° and compared with a high crystalline synthetic zeolite.

$$\% \text{ Crystallinity} = \frac{\sum \text{Area peaks sample}}{\sum \text{Area peaks reference}} \quad \text{Eq.1.}$$

The crystallite average size was estimated by using the Scherrer Equation (Eq. 2) where the  $\beta$  value was obtained from the highest intense peak.

$$\tau = K\lambda/\beta\cos\theta \quad \text{Eq.2}$$

The morphology of the samples was studied by scanning electron microscopy (SEM) technique on a SEM Magellan 400, FEI Company, without coating.

The thermal stability was determined by the Thermal Gravimetric Analysis (TGA) technique on a SETARAM TGA-DSC 1600 °C equipment. The sample was placed in an alumina crucible. The analysis was carried out from 25 °C to 800 °C, heating rate of 10 °C/min and He as carrier gas (15 mL/min). The data obtained were converted to derivate form of the TGA (DTGA) using the software of the equipment.

The quantification of the acid sites was carried out by the Ammonia Temperature Programmed Desorption (NH<sub>3</sub>-TPD) technique on a ChemBET TPR/TPD Quantachrom Analysis equipment. A known weight of zeolite was placed in the analysis cell. Then the zeolite was degassed at 250°C for 30 min and activated at 550 °C for 1 h with He as carrier (15 mL/min). Subsequently, a flow of 15 mL/min (5% NH<sub>3</sub>/He) passed through the cell and ammonia adsorption was carried out for 1 hour at 100 °C. Finally, the gas flow was changed to He (15mL/min) and heated to 850 °C at 9 °C/min. The signals were registered with a TCD detector. For the proper identification of the Lowry-Brønsted acid sites, a 1 M HCl solution (1:3 molar ratio) was applied with the ZSM-5 at room temperature for 3 hours. This treatment was performed to eliminate preferentially the extra framework aluminum species (EFAL).

#### *Catalyst performance in the MTH process*



The experiments were carried out in a stainless-steel fixed bed reactor at laboratory scale (see Figure 7), connected to an on-line Gas Chromatograph (Agilent 7890A series and a HP-PLOT-q column) with FID detector. The internal diameter of the reactor was 9.5 mm, in which about 650 mg of catalyst was charged. The catalyst was first activated at 500 °C with N<sub>2</sub> as carrier gas at 20 mL/min for 1 hour. Subsequently, the reactor was cooled down to 300 °C. Three different reaction conditions were studied: Condition A (300 °C and 1.2 L<sub>methanol</sub>/g<sub>cat</sub>), condition B (300 °C and 15 L<sub>methanol</sub>/g<sub>cat</sub>) and condition C (240 °C and 1.2 L<sub>methanol</sub>/g<sub>cat</sub>). All the experiments were done at atmospheric pressure (≈ 0.65 bar). Methanol was injected with a HPLC pump and external heated by heating tape, and mixed with N<sub>2</sub> (20 mL/min) prior sent to the reactor. HPLC grade methanol was used.

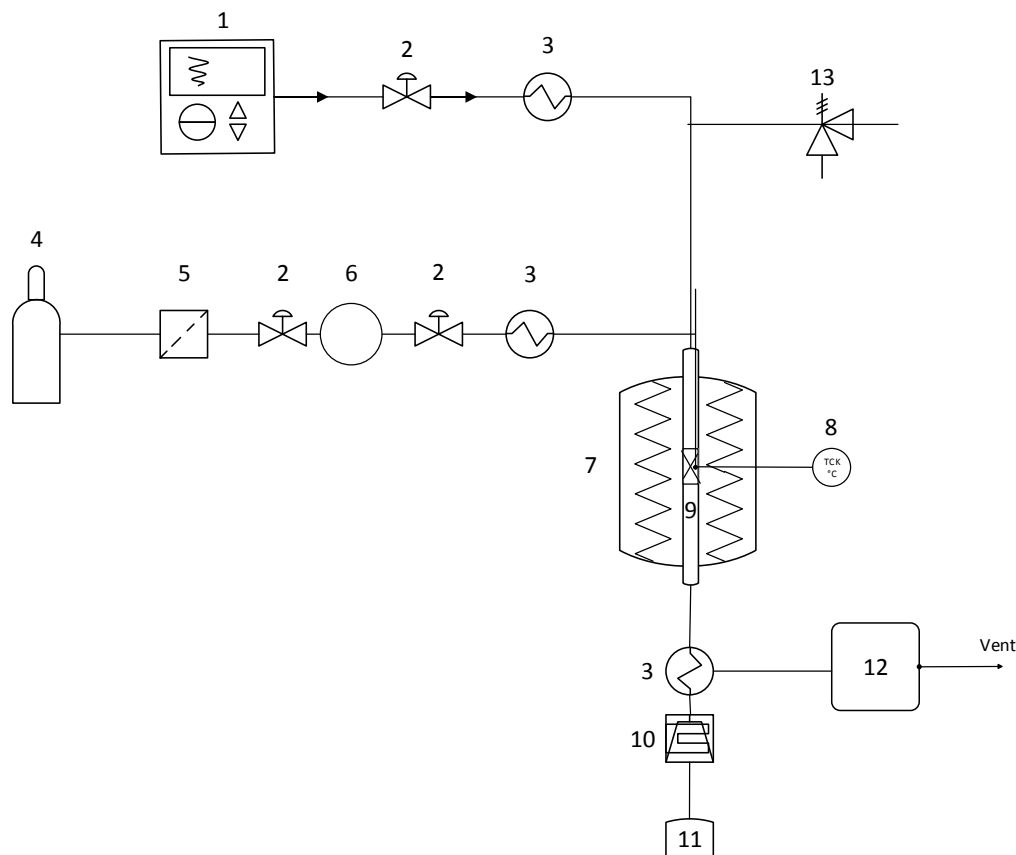


**Fig. 7.** Schematic overview of the fixed bed reactor. 1) HPLC pump, 2) Simple pass valve, 3) Heating cord, 4) Nitrogen gas cylinder, 5) Filter, 6) Mass flow controller (MFC), 7) Reactor furnace, 8) K type thermocouple, 9) Catalytic bed, 10) Condensation system, 11) Liquids trap and 12) Gas chromatograph.

Methanol conversion was calculated from the following equation [35]:

$$X = (F_{in} - F_{out}) / F_{in} \quad \text{Eq. 3}$$

Where  $F_{in}$  and  $F_{out}$  refers to molar flow of methanol at feed stream and after reaction, respectively. Product selectivity was calculated from the following equation [15]:

$$S_i = (A_i / R_{f_i}) * (1 / \sum (A_i / R_{f_i})) * 100 \quad \text{Eq.4}$$



Where  $A_i$  refers to the total area of the product “i” and  $Rf_i$  refers to the response factor for product “i” relative to methane. Some of the response factors were taken from Dietz et. al. [36].

## CONCLUSIONS

The acid treatment of diatomite with sulfuric acid reduces the concentration of elements such as Na, K, Ca, Mg, Fe and Al, transforming the diatomite into a good precursor for the synthesis of H-ZSM-5 zeolite. The obtained H-ZSM-5 zeolite shows high thermal stability, medium crystallinity degree and strong Lowry-Brønsted and Lewis acid sites. From a green chemistry perspective, the acid treatment of diatomite is extremely attractive as an opportunity for the zeolite manufacturing in industry, since it utilizes a natural raw material and would potentially be less expensive compared to traditional synthesis.

The use of the obtained H-ZSM-5 zeolite in the MTH process has showed good methanol conversion (>88 %) and high product selectivity of DME and olefins (mostly  $C_2^=$  and  $C_3^=$ ). By varying the reaction conditions (temperature and space velocity) the DME selectivity can be increased to as high as 95 %.

## ACKNOWLEDGMENTS

The authors acknowledge the financial support from The World Academy of Science (TWAS) and Swedish International Development Cooperation (SIDA). Ing. Mario Blanco is acknowledged for providing diatomite samples and facilitate the use of XRD equipment.

## REFERENCES

1. Arcoumanis, C., Bae, C., Crookes, R., Kinoshita, E. **2008**, *Fuel* 87, 1014–1030.
2. Avidan, A.A. **1988**, *Methane Conversion*, 307-323.
3. Sémeril, D., Dixneuf, P.H., Imamoglu, Y., Bencze, L. **2003**, *Novel Metathesis Chemistry: Well-Defined Initiator Systems for Specialty Chemical Synthesis, Tailored Polymers and Advanced Material Applications* 313-322.
4. Al-Megren, H., Xiao, T. *Petrochemical Catalyst Materials, Processes, and Emerging Technologies*, IGI Global, Engineering Science Reference, **2016**, Hershey, PA, USA, pp. 92-115.
5. Seo, G., Kim, J., Jang Catal, H. **2013**, *Surv. Asia*, 17, 103–118.
6. Lefevère, J., Mullens, S., Meynen, V., Van Noyen, J., **2014**, *Chemical Papers*, 68 (9), 1143–1153.
7. Narayanan, S., Sultana, A., Krishna, K. **1995**, *Catalysis Letters*, 34, 129-138.
8. Quan, Y., Li, S., Wang, S., Li, Z., Dong, M., Qin, Z., Chen, G., Wei, Z., Fan, W., Wang, J. **2017**, *ACS Appl. Mater. Interfaces*, 17 (9), 14899–14910.
9. Li, T., Liu, H., Fan, Y., Yuan, P., Shi, G., Bic, X.T., Bao, X., **2012**, *Green Chem.*, 14, 3255-3259.
10. Sanhueza, V., Kelm, U., Cid, R., López-Escobar, L. **2004**, *J. Chem. Technol Biotechnol.*, 79, 686–690.
11. Aguilar-Mamani, W., García, G., Hedlund, J., Mouzon, J. **2014**, *SpringerPlus*, 3, 292.
12. Xu, R., Pang, W., Yu, J., Huo, Q., Chen, J. *Chemistry of Zeolites and Related Porous Materials: Synthesis and Structure*, John Wiley & Sons, **2007**, Singapore, pp. 41-72.
13. Pavlova, A., Trinh, T.T., Van Santen, R.A., Meijer E.J. **2013**, *Phys. Chem. Chem. Phys.*, 15, 1123-1129.
14. Narayanan, S., Sultana, A., Thinh Le, Q., Auroux, A. **2009**, *Catalysis Today*, 142, 90–97
15. Lónyi, F., Valyon, J. **2001**, *Microporous and Mesoporous materials*, 47, 293-301.
16. Hunger, B., Hoffmann, J., Heitzsch, O., Hunger, M. **1990**, *Journal of Thermal Analysis*, 36, 1379-1391.
17. Nováková, J., Kubelková, D., Habersberger, K., Dolejšek, Z. **1984**, *J. Chem. Soc., Faraday Trans. 1*, 80, 1457-1465.
18. Takeuchi, M., Tsukamoto, T., Kondo, A., Matsuoka, M. **2015**, *Catal. Sci. Technol.*, 5, 4587-4593.
19. Lu, C., Liu, T., Shi, Q., Li, Q., Xin, Y., Zheng, L., Zhang, Z. *Scientific Reports, published online*, 7, 3300.
20. Huang, M., Kaliaguine, S., Auroux, A. *Zeolites: A Refined Tool for Designing Catalytic Sites*, 97, Elsevier, **1995**, Amsterdam, pp. 311-318.
21. Bernardon, C., Osman, M.B., Laugel, G., Louis, B., Pale, P. **2016**, *Comptes Rendus Chimie*, 1-10.
22. Sandoval-Díaz, L., González-Amaya, J., Trujillo, C. **2015**, *Microporous and Mesoporous Materials*, 215, 229-243.
23. Wang, Q.L., Giannetto, G., Guisnet, G. **1991**, *Journal of Catalysis*, 130, 471-482.
24. Smieskova, A., Bocan, J., Hudec, P., Zidek, Z. 1994, *Zeolites*, 14, 553-556.
25. Horňáček, M., Hudec, P., Nociar, A., Smiesková, A., Jakubik, T. **2010**, *Chemical Papers*, 64 (4), 469–474
26. Deka, R. CH. **1998**, *Indian Journal of Chemical Technology*, 6, 109-123.
27. Huang, J., Jiang, Y., Marthala, Y.R.R., Thomas, B., Romanova, E., Hunger, M. **2008**, *J. Phys. Chem. C*, 112, 3811-3818.
28. Smail, H.A., Rehan, M., Shareef, K.M., Ramli, Z., Nizami, A., Gardy, J. **2019**, *Chem. Engineering*, 3, 35.
29. Chua, S., Yangb, L., Guoa, X., Donga, L., Chena, X., Lia, Y., Mua, X. **2018**, *Molecular Catalysis*, 445, 240–247.
30. Stöcker, M. **1999**, *Microporous and Mesoporous Materials*, 29, 3–48.
31. Chen, J., Li, C., Yuan, S., Xu, Y., Wei, Q., Wang, Y., Zhou, J., Wang, M., Zhang, Y., He, S., Xua, Z. **2014**, *Sci. Technol.*, 4, 3268-3277.



32. Chang, C.D. **1988**, *Methane Conversion*, 127-143.
33. Castellanos-Beltran, I., Palla, G., Lavoie, J. **2018**, *Chem. Sci. Eng.*, 12 (2), 226–238.
34. García Mendoza, J.G., Synthesis of zeolites from Bolivian raw materials for catalysis and detergency applications, licentiate thesis, Luleå University of Technology, Department of Civil, Environmental and Natural Resources Engineering.
35. Andersson, R., Boutonnet, M., Järås, S. **2012**, *Journal of Chromatography A*, 1247, 134– 145.
36. Dietz, W.A. **1966**, Response factors for gas chromatographic analysis, *Journal of Gas Chromatography*.  
[https://www.che.psu.edu/faculty/Rioux/group/group\\_info/references/response\\_factors\\_for\\_gas\\_chromatographic\\_analyses.pdf](https://www.che.psu.edu/faculty/Rioux/group/group_info/references/response_factors_for_gas_chromatographic_analyses.pdf),  
Access date: 19/08/2019.